Cell Death and Differentiation (2008) 15, 123–133

www.nature.com/cdd

Isolation and characterization of a murine resident liver stem cell

A Conigliaro[1], M Colletti[1], C Cicchini[1,2], MT Guerra[2,3], R Manfredini[4], R Zini[4], V Bordoni[2], F Siepi[2], M Leopizzi[5], M Tripodi*[,1,2] and L Amicone[1]

Increasing evidence provides support that mammalian liver contains stem/progenitor cells, but their molecular phenotype, embryological derivation, biology and their role in liver cell turnover and regeneration remain to be further clarified. In this study, we report the isolation, characterization and reproducible establishment in line of a resident liver stem cell (RLSC) with immunophenotype and differentiative potentiality distinct from other previously described liver precursor/stem cells. RLSCs, derived from fetal and neonatal murine livers as well as from immortalized hepatocytic MMH lines and established in lines, are Sca +, CD34−, CD45−, α-fetoprotein + and albumin−. This molecular phenotype suggests a non-hematopoietic origin. RLSC transcriptional profile, defined by microArray technology, highlighted the expression of a broad spectrum of 'plasticity-related genes' and 'developmental genes' suggesting a multi-differentiative potentiality. Indeed, RLSCs spontaneously differentiate into hepatocytes and cholangiocytes and, when cultured in appropriate conditions, into mesenchymal and neuro-ectodermal cell lineages such as osteoblasts/osteocytes, chondrocytes, astrocytes and neural cells. RLSC capability to spontaneously differentiate into hepatocytes, the lack of albumin expression and the broad differentiative potentiality locate them in a pre-hepatoblast/liver precursor cells hierarchical position. In conclusion, RLSCs may provide a useful tool to improve liver stem cell knowledge and to assess new therapeutic approaches for liver diseases.
Cell Death and Differentiation (2008) **15,** 123–133; doi:10.1038/sj.cdd.4402236; published online 12 October 2007

Introduction

The identification, isolation, *in vitro* expansion and therapeutic use of stem cells from various tissues represent the greatest current challenges in tissue engineering and regenerative medicine. Up to date, formidable progresses in handling hematopoietic, mesenchymal[1,2] and simple epithelia stem cells[3] have been made, and therapeutic protocols aiming at the repopulation of depleted bone marrow, the regeneration of ischemic myocardium[4] and the reconstitution of damaged corneal epithelium[5,6] are already available. On the other hand, the possibility to engineer many other tissues, in particular complex epithelia, is still very limited. Successful approaches for stem cells utilization have been substantially based on empirical attempts to identify specific cell markers, anatomical compartments for cell isolation, appropriate conditions for *in vitro* culture and *in vivo* cell transfer.

In the case of liver, the ability of fully differentiated hepatocytes to give rise *in vivo* to cellular progeny that replace cell loss is well known. The 'staminal capability' of differentiated hepatocyte has encouraged the development of hepatocyte transplantation protocols that, unfortunately, yielded only partially effective therapeutic benefits.[7] When hepatocyte proliferation is impaired, the expansion of a limited compartment of progenitor cells, the oval cells, becomes recognizable.[8] This mix population of cells expresses markers common to hepatocytes and cholangiocytes and gives rise to both liver epithelial cell lineages.[9] Similarly, bipotential precursor cells, able to differentiate and colonize diseased liver in animal models, have been isolated from rodent and human livers.[10–12] Other extra and intra-hepatic precursor/stem cell compartments have also been proposed. The excitement on an 'extra-liver' hepatic stem cell, derived from studies showing *trans*-differentiation ability of bone marrow-derived hematopoietic stem cells into hepatocytes,[13–15] has been narrowed by its limited contribution to liver regeneration and by data highlighting as transplanted cells, observed in the recipient liver, were the product of cell fusion rather than *trans*-differentiation.[16–18] Regarding the 'resident' liver stem cell, two recent interesting reports describe pluripotent progenitor populations isolated from fetal (human fetal liver multipotent progenitor cell, hFLMPC)[19] and adult (human liver stem cell, HLSC)[20] livers. The HLSCs, proposed as mesenchymal liver population, and the hFLMPCs, proposed as mesenchymal-

[1]Department of Cellular Biotechnologies and Hematology, Istituto Pasteur-Fondazione Cenci Bolognetti, University 'La Sapienza', Rome, Italy; [2]National Institute for Infectious Diseases L Spallanzani, IRCCS, Rome, Italy; [3]Department of Physiology and Biophysics, Federal University of Minas Gerais, Belo Horizonte- Minas Gerais, Brazil; [4]Department of Biomedical Sciences, University of Modena and Reggio Emilia, Modena, Italy and [5]Department of Experimental Medicine, University 'La Sapienza', Rome, Italy

*Corresponding author: M Tripodi, Dipartimento di Biotecnologie Cellulari ed Ematologia, Sezione di Genetica Molecolare, Università La Sapienza, Viale Regina Elena 324, Rome 00161, Italy. Tel: +39 06 4461387; Fax: +39 06 4462891; E-mail: tripodi@bce.uniroma1.it

Keywords: sca1 antigen; self-renewal; microArray; differentiative pluripotency; liver stem cell lines

Abbreviations: α−FP, α-fetoprotein; BC, basal conditions; CC, chondrogenic conditions; dpc, days post coitum; GFAP, glyal fibrillar acid protein; HC, hepatocyte conditions; MetE14, cyto-Met transgenic embryo 14 dpc; MetNBD6, cyto-Met transgenic mouse 6 days newborn; MMH, met murine hepatocyte; NC, neurogenic conditions; OC, osteogenic conditions; RLSC, resident liver stem cell; wtE14, wild type embryo 14 dpc; ZO-1, zonula occludens 1

Received 04.4.07; revised 03.9.07; accepted 07.9.07; Edited by G Cossu; published online 12.10.07

epithelial transitional cells, displayed the ability to differentiate into hepatocyte and cholangiocyte as well as into several mesenchymal lineages.

We have previously characterized and immortalized bipotential precursor cell line (Palmate cells) isolated from immortalized non-tumorigenic hepatocytic cell lines (MMH) derived from embryonic livers of cyto-Met transgenic mice.[10,21,22] On the basis of this evidence, several successful attempts to isolate and manipulate liver bipotential cells from many mouse inbred strains have been reported.[11,23] Considering that an immortalized cell line is an invaluable tool for *in vitro* studies of molecular mechanisms controlling stem cell maintenance and differentiation, we aimed at the isolation and establishment in line of a resident liver stem cell.

Here we describe how non-tumorigenic stable stem cell lines are reproducibly obtainable from murine liver explants at various stages of development. These cells, named RLSCs from resident liver stem cells, in their undifferentiated state, display a typical stemness expression profile, self-renewing capability and a multilineage differentiation potentiality. We showed that RLSCs, under appropriate culture conditions, give rise to progeny that expresses specific markers for polarized hepatocytes, cholangiocytes, osteoblasts, chondrocytes and neural cells.

Results

Derivation and establishment of RLSCs from liver explants. Primary cultures were prepared from livers of wild type embryos 14 days post coitum (dpc) (wtE14), cyto-Met transgenic embryos 14 dpc (MetE14) and cyto-Met transgenic mice 6 days after birth (MetNBD6). Table 1 summarizes the cell events obtained. Out of seven

Table 1 Cumulative evaluation of RLSCs derivation

Primary cultures	Number of colonies	Clones with palmate morphology	Time for colony emergence	Immortalized RLSC lines	Efficiency of tumor formation in nude mice
WT E14	25	4	7 weeks	3	$<1\times10^{-6}$
Met E14	30	4	4 weeks	3	$<1\times10^{-6}$
Met NB-D6	15	2	4 weeks	1	$<1\times10^{-6}$

The table summarizes the immortalization events obtained from primary cultures of wtE14, MetE14 and MetNBD6 livers. In each case the primary cultures were seeded at high density in a collagen treated 10 cm dish

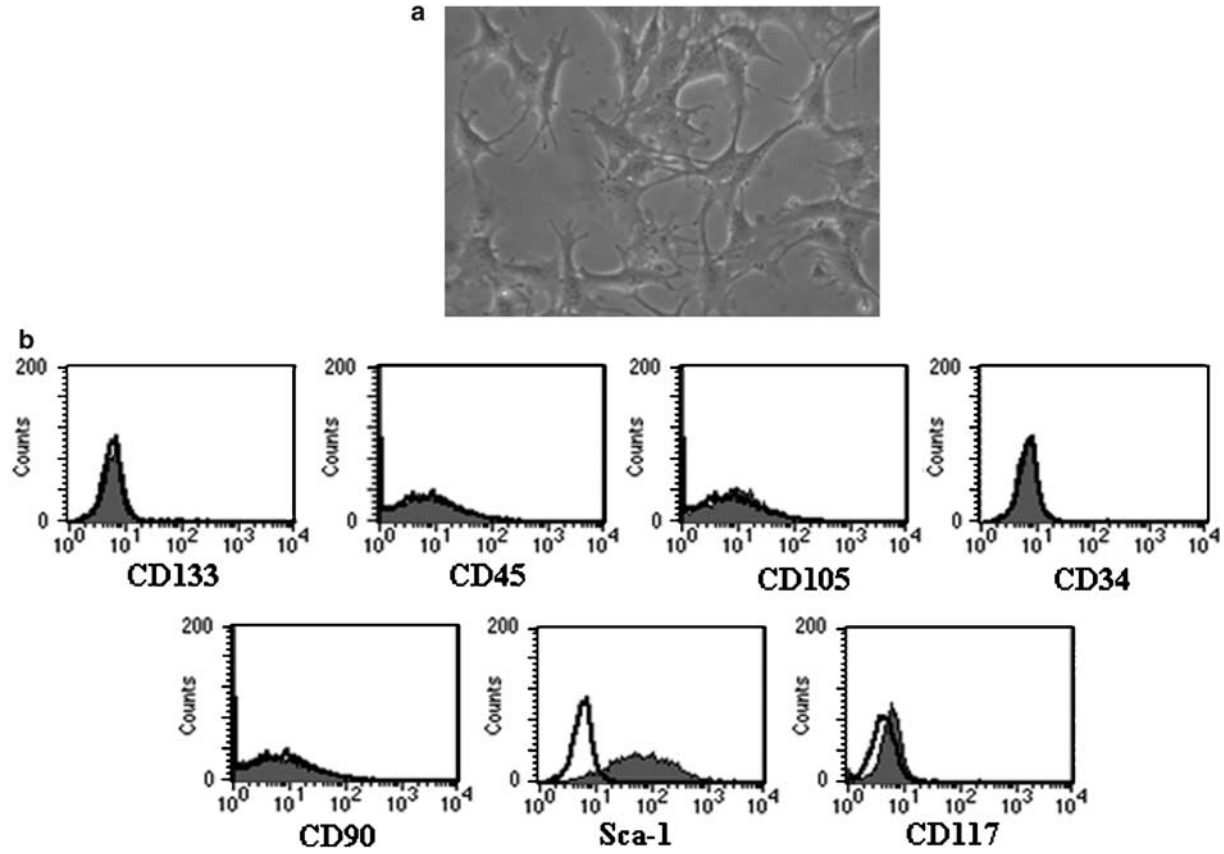

Figure 1 Cell surface phenotype of RLSCs. (**a**) Phase-contrast micrograph of a representative RLSC line showing the typical 'palmate' morphology. (**b**) FACS analysis for the indicated surface molecules. Filled curves: specific antibody staining; unfilled curves: isotype control antibody. Data are representative of three separate experiments

established RLSC lines, three (WTE14/1, MetE14/3 and MetNBD6/1) have so far been kept in culture for more than 12 months and from them individual clones, by limiting dilution (see Materials and Methods), were derived (Figure 1a). Three clones, one for each line, were immunophenotyped as Sca1+, CD45−, CD34−, CD117− and CD133− (Figure 1b) and used for further described characterization.

RLSC differentiation toward liver epithelial cell lineages. Firstly, RLSCs were tested for their capability to differentiate into liver epithelial cell lineages both *in vitro* and *in vivo*. To ascertain the *in vitro* ability to differentiate along the hepatocytic lineage, the three different RLSC clones were repeatedly grown to confluence and subcultured in Hepatocyte Conditions (HC). After an average of six passages, RLSCs acquired a hepatocyte-like morphology (cuboidal and tightly packed) independently of cell confluence. The morphological changes corresponded to the acquisition of epithelial polarization and hepatocyte differentiation as revealed by the immunofluorescence analysis. Figure 2a shows that the polarity markers Zonula Occludens 1 (Zo-1) and E-cadherin (E-cad) are localized to the membrane and that Albumin and Hepatocyte Nuclear Factor (HNF)-4α are expressed in more than 90 percent of the cells. RT-PCR analysis extended the observations to other liver enriched transcriptional factors and liver products (Figure 2b).

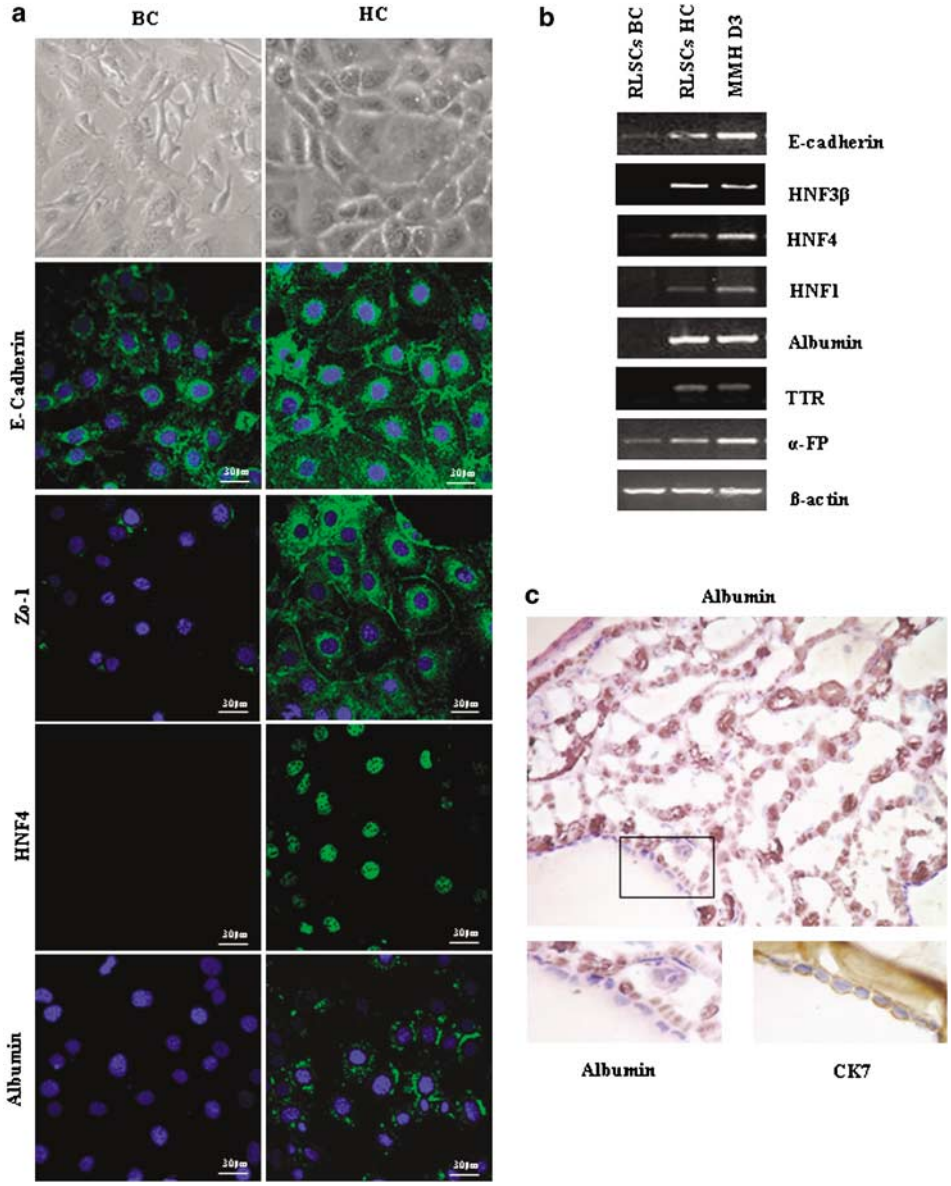

Figure 2 RLSCs differentiate toward hepatic lineages. (**a**) Phase-contrast micrographs and confocal immunofluorescence analysis for the polarization markers E-cad and Zo1, for the liver product Albumin and for the hepatocyte-specific transcription factor HNF4alpha, of WT E14/1clone cultured in basal conditions (BC) and in hepatocyte conditions (HC) for 21 days. Nuclear staining was performed with toppro3. Similar results have been obtained with the other two clones. (**b**) Comparative RT-PCR analysis, for the indicated liver specific transcriptional factors and products, of RLCSs cultured in BC and HC for 21 days and, as control, of MMH-D3 line. (**c**) Immunohistochemical findings (staining for Albumin and CK7) of the engineered hepatic-like tissue obtained 60 days after RLCSs subcutaneous transplantation: the albumin-positive cells form epithelial trabeculae while CK7 positive/albumin negative cells delimit empty spaces that recall bile ducts. Nuclear staining was performed with ematossilin

To test *in vivo* the capability to differentiate along the hepatic lineages, RLSCs were injected into neovascularized subcutaneous cavities opportunely prepared in nude mice. As shown in Figure 2c, these cells differentiate along both parenchymal liver lineages, acquiring a striking spatial organization with albumin-positive cells recalling the typical liver epithelial trabeculae and CK-7 positive cells defining bile duct-like structures. Remarkably, the expressions of albumin (hepatocyte marker) and CK7 (cholangiocyte marker) were mutually exclusive.

Gene expression profile. To define molecular phenotype of the RLSCs, we assessed the transcriptome profile using Affymetrix Mouse430_2 GeneChip array. For this analysis, we chosen MetE14/3 and the WTE14/1 RLSC lines. The expression profiles were compared to that of the previously characterized hepatocytic differentiated cell line, MMH-D3.[21] All the data have been deposited in the Gene Expression Omnibus MIAME compliant public database, at http://www.ncbi.nlm.nih.gov/geo (Table S1 of Supplementary Data). Using DAVID TOOL 2.1 β, we assessed which GO categories were significantly modulated. As detailed in Table S2 of Supplementary Data, many genes belonging to biological process GO categories, such as 'establishment and/or maintenance of chromatin architecture', 'DNA packaging', 'chromatin assembly or disassembly,' were significantly upregulated in RLSCs. As reported in Table 2 (chromatin remodeling genes), the chromatin regulators belonging to the SWI/SNF ATPase family Smarcd3, a helicase of the snf2/rad54 family (Chd3), a deacetylase (Sirt1) and the deacetylase interactor Sap18, a DNA methyltransferase (Set7) and two regulators of chromatin assembly and nuclear organization (Cbx2, Chc1l) exhibited an upregulated expression in RLSCs. Concerning genes belonging to tissue development GO categories, while those controlling the endoderm are expressed in both cell lines, GO categories involved in other tissue development, such as 'skeletal development', 'nervous system development', 'muscle development', 'embryonic development' and 'cartilage development,' were upregulated in RLSCs (see Table S2 in Supplementary Data). As shown in Table 2 (Stem cell and differentiation markers), the brain specific transcription factors Ebf3 and Zfp207, the transcription factor Twist2, implicated in osteoblastic differentiation and the receptor for WNT proteins Fzd1, involved in chondrocyte differentiation, displayed an upregulation in RLSCs. Moreover, Table 2 shows as genes considered hallmarks of embryonal and adult stem cells, such as Bmi1, Sca1, Notch1, Hoxa10, Hoxa9, Meis1 and, surprisingly, markers specific for all of the three endodermal (Foxa1), mesodermal (CNN1) and ectodermal (nestin, Enc1) stem cells were upregulated in RLSCs. We next validated and extended the significance of microArray data by performing a quantitative RT-PCR analysis on a subset of genes for all of the three clones. As shown in Figure 3, we found a coherent expression pattern among the three RLSC clones with respect to control MMH-D3 cells. Overall, these data suggest that the capability of RLSCs to differentiate along the hepatic lineages is based on the expression of a broad number of 'plasticity related genes'. Moreover, the RLSCs were found to express a number of genes related to multidifferentiative programs thus suggesting that their plasticity may not be restricted to the hepatic lineages. This prompted us to manipulate them toward other cell lineages. By means of soluble factors and culture conditions mutuated from the literature, we tested the capability of the three RLSC lines to differentiate along the osteoblastic, chondrocytic and neuronal lineages.

Table 2 Genes increased in RLSCs belonging to chromatin remodeling and stem cell marker categories

ProbeSet ID	Gene title	Gene symbol	LocusLink	Met E14/3 RLSCs vs MMH-D3 SLR	WT E14/1 RLSCs vs MMH–D3 SLR
Chromatin remodeling genes					
1434116_at	Chromobox homolog 2 (Drosophila Pc class)	Cbx2	12416	1.1	1.8
1416389_a_at	Chromosome condensation 1-like	Chc1l	105670	1.8	2.3
1428466_at	Chromodomain helicase DNA-binding protein 3	Chd3	216848	1.7	1
1449480_at	Sin3-associated polypeptide 18	Sap18	20220	1.3	1.3
1435437_at	SET domain-containing protein 7	Set7	73251	2.3	1.6
1418640_at	Sirtuin 1 ((silent mating type information regulation 2, homolog) 1 (*S. cerevisiae*)	Sirt1	93759	1	1
1418467_at	SWI/SNF related, matrix associated, actin-dependent regulator of chromatin, subfamily d, member 3	Smarcd3	66993	5.8	4.3
Stem cell and differentiation markers					
1428349_s_at	Early B-cell factor 3	Ebf3	13593	3	6.2
1448925_at	Twist homolog 2 (Drosophila)	Twist2	13345	5.1	1.5
1437284_at	Frizzled homolog 1 (Drosophila)	Fzd1	14362	2.2	3.8
1438294_at	Spinocerebellar ataxia 1 homolog (human)	Sca1	20238	2.4	1.1
1418634_at	Notch gene homolog 1 (Drosophila)	Notch1	18128	1.3	1.2
1448733_at	B lymphoma Mo-MLV insertion region 1	Bmi1	12151	1.6	1.3
1431475_a_at	Homeo box A10	Hoxa10	15395	2	1
1455626_at	Homeo box A9	Hoxa9	15405	2.9	1
1450992_a_at	Myeloid ecotropic viral integration site 1	Meis1	17268	2.2	1
1418496_at	Forkhead box A1	Foxa1	15375	8.1	1
1417917_at	Calponin 1	Cnn1	12797	4.2	1.5
1420965_a_at	Ectodermal-neural cortex 1	Enc1	13803	1.1	2
1449022_at	Nestin	Nes	18008	5.9	1.9

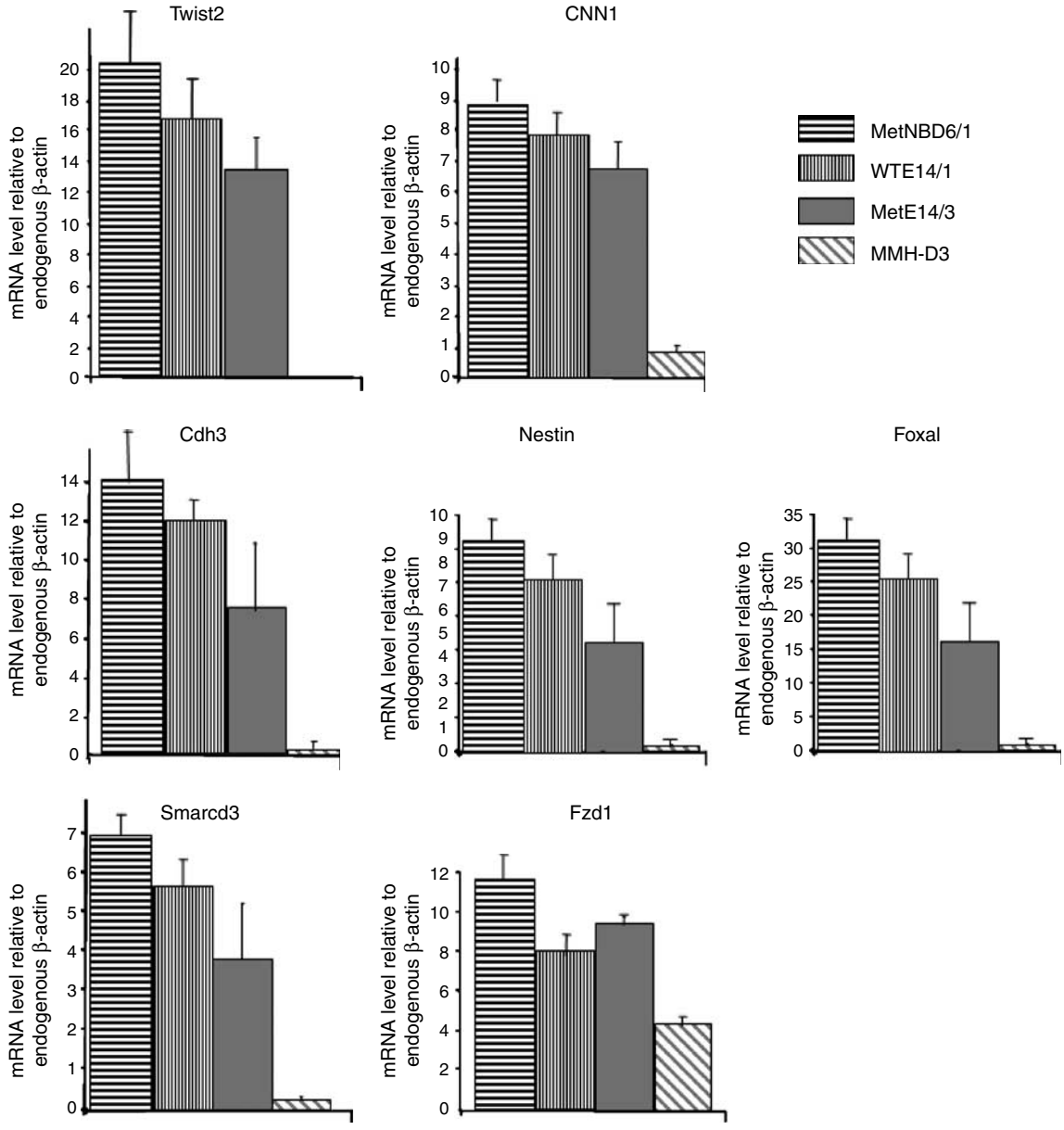

Figure 3 RLSCs transcriptional profile. Validation of MicroArray gene expression data by real-time RT-PCR (qRT-PCR). The analysis for the indicated genes was performed on RLSCs (WTE14/1, MetE14/3 and MetNBD6/1 clones) cultured in basal conditions and on MMH-D3. The RT-PCR results were calculated by Delta-Delta CT Method

RLSC differentiation toward osteoblastic lineage. RLSCs were induced to differentiate along the osteoblastic lineage under Osteogenic Conditions (OC). Interestingly, within 14 days OC induced a change in cellular morphology parallel with the induction of osteoblast/osteocyte specific genes, as revealed by RT-PCR analysis for Osteocalcin, Parathormon receptor, Periostin, Osteopontin, Alkaline Phospatase 2 and Ibfp (Figure 4a); moreover, 70–80 percent of cells became positive for Alkaline Phosphatase staining and, at longer time (3 weeks), underwent CaPO4 mineralization process, revealed by Red Alizarin staining (Figure 4b). These data provide evidences for the osteoblast/osteocyte differentiative potentiality of RLSCs.

RLSC differentiation toward chondrocyte lineage. We next induced RLSCs to differentiate along the chondrocyte lineage under chondrogenic conditions (CC), chosen in accord with standard protocols for culture of primary chondrocytes. Cells, within 21 days in CC, form a suspended compact micromass '*per se*' recapitulating the process of chondrogenesis and chondrocyte maturation. To unveil a coherent molecular phenotype, pellets were analyzed for transcripts and products of chondrocyte specific genes. RT-PCR analysis demonstrated the Aggrecan and Collagen-II expression (Figure 4c); immunohistochemical and histochemical analyses showed a 30 percent of chondrocyte-like cells expressing collagen II (Figure 4d)

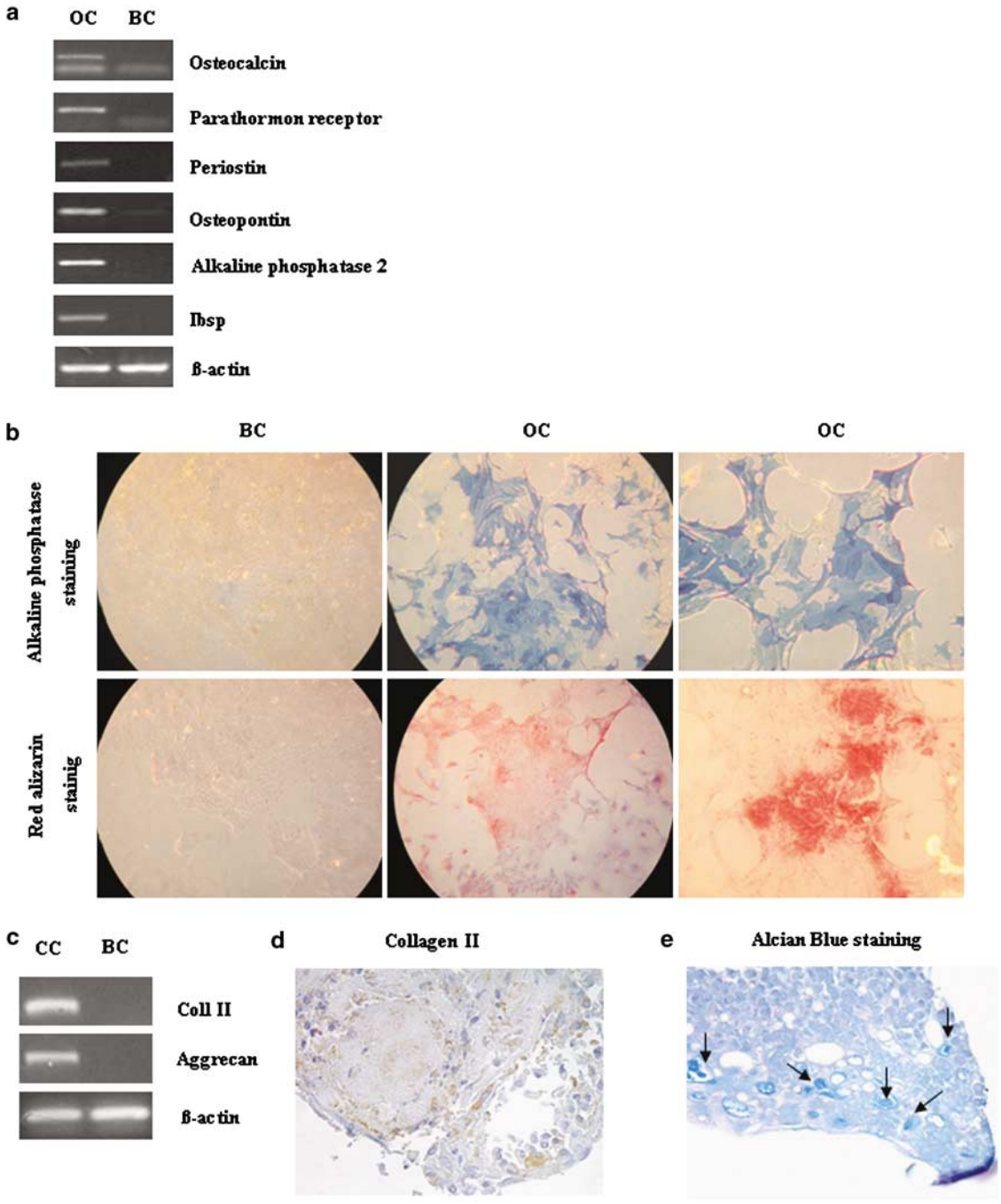

Figure 4 RLSCs differentiate toward osteoblast/osteocyte and chondrocyte lineages. (**a**) RT-PCR analysis for osteoblast/osteocyte-specific markers. RLSCs cultivation for 14 days in osteogenic conditions (OC) induced the transcription of the indicated osteoblast/osteocyte specific genes. As control, the analysis was performed on undifferentiated RLSCs cultured in basal conditions (BC) for the same time. (**b**) Histochemical analysis for osteoblast/osteocyte-specific markers. MetNBD6/1 clone cultivated for 14 days in OC became positive for alkaline phosphatase staining; RLSCs cultivated for 21 days in OC underwent CaPO4 mineralization process evidenced by Red Alizarin staining. As control, the analyses were performed on RLSCs cultured in BC for the same time. Similar results have been obtained with the other two clones. (**c**) RT-PCR analysis for chondrocyte-specific markers. MetNBD6/1 clone cultivation for 14 days in chondrocyte conditions (CC) induced the transcription of the indicated chondrocyte-specific genes. As control, the analysis was performed on undifferentiated RLSCs cultured in BC for the same time. Similar results have been obtained with the other two clones. (**d** and **e**) Immunohistochemical and histochemical analyses for chondrocyte-specific markers. MetNBD6/1 clone cultured as micro-pellets showed chondrocyte-like cells positive for collagen type II and lodged in lacunae (arrows) embedded in Alcyan Blu positive matrix. Similar results have been obtained with the other two clones

lodged in lacunae embedded in Alcyan Blu positive matrix (Figure 4e). These data provide evidence for the chondrocyte differentiative potential of RLSCs.

RLSC differentiate toward neural cell lineages. We next induced RLSCs to differentiate along the neural cell lineages under neurogenic conditions (NC) mutuated from neural

stem cells culture and differentiation protocols. In particular, for neurogenic induction, RLSCs were cultured as spheres and then seeded on collagen, where cells grew as monolayer, or on Matrigel, where cells spread out (Figure 5a). Both conditions caused upregulation of neuron-related genes, although with differences. The RT-PCR analysis, in fact, revealed that cells grown on matrigel downregulated the neuronal precursor markers Nestin and NPas1 and upregulated the neuronal specific genes Fgf9 and NeuroD2, while cells grown on collagen coexpress the neuronal specific genes Ngn1 and NeuroD2 with Nestin and NPas1 (Figure 5b). Finally, to further induce the neuronal differentiation, spheres were mechanically dissociated and cells cultivated at low density on matrigel. After 14 days, 50–60 percent of cells were found positive for the astrocyte marker Glyal Fibrillar Acid Protein (GFAP) and after 21 days, 20–30 percent of cells, for β III tubulin (Figure 5c). These data provide evidence for initial neural differentiation of RLSCs. Notably, RLSCs derived from liver explants of a MetNBD6 mouse failed to differentiate along neuro-ectodermal lineages.

Discussion

In this work, we describe the reproducible isolation and characterization of resident liver stem cells with self-renewal capability and competence to differentiate into hepatic parenchymal cells and, when instructed by specific culture conditions, into mesenchymal and neuroectodermal lineages.

These cells, established in several non-tumorigenic clonal cell lines, differ from other previously described liver stem/precursor cells. RLSCs, in fact, do not express albumin, a liver product normally present in other liver precursor cells, such as hepatoblasts and oval cells, as well as in the recently described human liver precursor/stem cells, HLSCs.[20] Moreover, RLSCs express the liver tissue-specific protein α-fetoprotein (αFP), which is considered a marker of early hepatocyte precursors and is not expressed in hepatic mesenchymal stem cells and in the recently reported human fetal liver multipotent progenitor cells, hFLPMs.[19] RLSCs do not express CD45 and CD34 hematopoietic stem cell markers, suggesting that they do not derive from circulating hematopoietic cells. The transcriptional profile of RLSCs mirrors and probably explains their plasticity. Undifferentiated RLSCs coexpress a wide range of mesenchymal (e.g. calponin 1), endodermal (e.g. FoxA1 and αFP) and neuroectodermal (e.g. nestin) stem cell markers together with several plasticity-related genes (chromatin remodeling genes) widely considered crucial for the activation of stem cell genetic programs.[24–26]

RLSCs differentiate into hepatic epithelia spontaneously. Notably, HCs being free of differentiative cytokines (e.g.

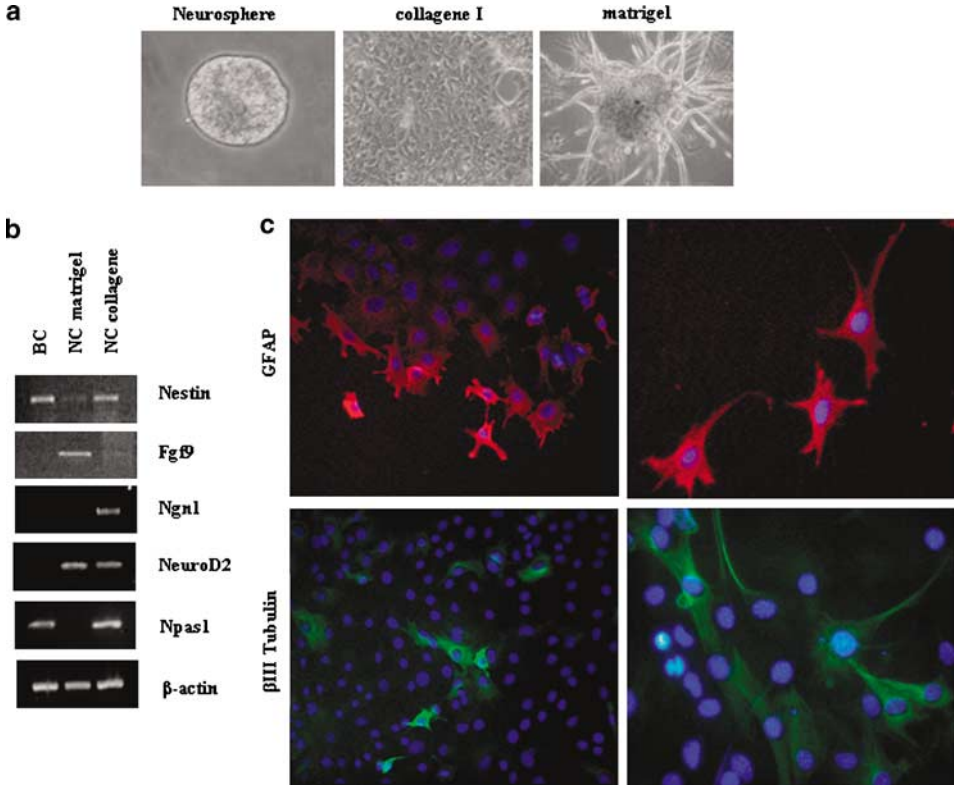

Figure 5 RLSCs differentiate toward the neuro-ectodermal cell lineages. (**a**) Phase-contrast micrographs of MetE14/3 clone, cultured as neurospheres and subsequently seeded on collagen, grew as monolayer and on matrigel, where the cells spread out. (**b**) RT-PCR analysis for neuronal-specific markers. MetE14/3-spheres cultivated on Matrigel downregulated the neuronal precursor markers Nestin and NPas1 and upregulated the neuronal-specific genes Fgf9 and NeuroD2; MetE14/3-spheres cultivated on collagen upregulate the neuronal-specific genes Ngn1 and NeuroD2. As control, the analysis was performed on MetE14/3 cultured on BC. Similar results have been obtained with WTE1 4/1. (**c**) Immunostaining for the neural markers of MetE14/3-spheres mechanically dissociated and cultivated at low density in matrigel. The cells became positive for the astrocyte marker GFAP after 14 days of culture and after 21 days for β III tubulin. Similar results have been obtained with WTE14/1

Oncostatin-M and HGF) do not induce hepatocyte and/or cholangiocyte markers in CD34 + bone marrow-derived cells (data not shown). This intrinsic differentiation program distinguishes RLSCs from liver mesenchymal and haematopoietic stem cells.

RLSCs differentiate into chondrocytes and osteoblast/osteocytes, as determined by observations, at morphological, transcriptional and immunohistochemical levels highlighting the acquisition of tissue-specific markers.

Interestingly, RLSCs grow as spheres and express typical markers of neuronal and astrocytic cells. In fact, RLSCs respond to specific culture conditions with a morphological transition that parallels the expression of astrocyte-specific GFAP and neuron-specific β III tubulin, expressed in different cells in a mutually exclusive fashion. Even if the cell morphology suggests only an initial neural differentiation process, we believe that the observed neurogenic behavior represents a novel trait of plasticity attributed to a resident liver stem/precursor cell. While all the other differentiated phenotypes measured and described were identical for the three RLSC lines, regardless of the genotype and the stage of isolation, the neurogenic potentiality was not found in RLSCs isolated from the liver of days 6 newborn mouse, suggesting a more strict meso-endodermal commitment of RLSCs after birth.

Finally, the RLSC self-renewal and asymmetric division capability was supported not only by the mere observation of an expansion and long-term maintenance of undifferentiated cells, but also by the possibility to re-isolate them from differentiated MMH lines[21] maintained in culture for more than 40 populations (data not shown).

In conclusion, RLSCs may contribute to elucidation of many aspects of stem cell biology, liver development and hepatocyte differentiation. In particular, they provide an *in vitro* system for the identification of critical microenviromental factors involved in stem cell maintenance, expansion and lineage-specific differentiations.

Materials and Methods

Animals. Mice (Charles River Laboratories, Lecco, Italy) received human care and the procedures involving them were conducted in conformity with the criteria outlined in the 'Guide for the Care and Use of Laboratory Animals' prepared by the National Academy of Sciences and published by the National Institutes of Health (NIH publication 86–23 revised 1985).

Primary hepatocyte culture. Primary cultures were performed in accord with previously described protocol (Amicone, 1997[21]) with some modifications. Briefly, livers from 14.5 dpc embryos and 6 days newborns were dissected, mechanically dissociated using a Potter glass homogenizer and plated at high density on collagen I (Transduction Laboratories, Lexington, UK) coated dishes (Falcon-BD, Franklin Lakes, NJ, USA) in RPMI-1640, supplemented with 10% fetal bovine serum (FBS) (Gibco, Carlsbad, CA, USA), 50 ng/ml epidermal growth factor, 30 ng/ml insulin like growth factor II (PeproTech Inc, Rocky Hill, NJ, USA), 10 μg/ml insulin (Roche, Mannheim, Germany), 2 mmol/l L-glutamine, 100 μ/mL penicillin and 100 μg/ml streptomycin (Gibco). After 12–24 h, the cultures were washed to remove all unattached cells, including red blood cells and the medium replaced. The cultures were maintained without transfer for several weeks with medium replacement twice a week. Within 4 weeks of culture the majority of cells died, and within 6 weeks colonies with distinct cell morphology became visible; cloning rings were placed around cell colonies allowed to transfer the clones with palmate morphology that were subcultured in Dulbecco's modified Eagle's medium (DMEM) containing 10% FBS (basal medium) on collagen I-coated dishes and frozen after ~50 cell generations. Subsequently, to obtain clonal cell lines, we performed limiting dilution seeding cells in a microtitration plate at a concentration of 0.1 cell per well^{-1}. Passages are calculated from initial thawing.

RNA extraction and Microarray data analysis. Total RNA from each sample was extracted using RNeasy Mini Kit (Qiagen, Valencia, CA, USA) following the protocol supplied by the manufacturer. Disposable RNA chips (Agilent RNA 6000 Nano LabChip kit, Agilent Technologies, Waldbrunn, Germany) were used to determine the concentration and purity/integrity of RNA samples using Agilent 2100 Bioanalyzer.

One-cycle target labeling assays, as well as the Affymetrix Mouse430_2 GeneChip arrays hybridization, staining and scanning, were performed using Affymetrix standard protocols (Affymetrix, Santa Clara, CA, USA).

Briefly, biotin-labeled target synthesis was performed, starting from 5 μg of total cellular RNA, according to the protocol supplied by the manufacturer (Affymetrix, Santa Clara, CA, USA). Labeled cRNA was purified using Affymetrix GeneChip Sample Cleanup Module and fragmented (15 μg) as described in the Affymetrix GeneChip protocol. Disposable RNA chips (Agilent RNA 6000 Nano LabChip kit, Agilent Technologies, Waldbrunn, Germany) and Agilent 2100 Bioanalyzer were used to determine the cRNA concentration/quality as well as to optimize the cRNA fragmentation.

The fragmented cRNA was then hybridized to an identical lot of Affymetrix Mouse430_2 GeneChip arrays for 16 h. GeneChips were washed and stained using the instrument's standard Eukaryotic GE WS2v5 protocol, using antibody-mediated signal amplification. GeneChip were finally scanned using the Affymetrix GeneChip scanner 3000, enabled for high-resolution scanning.

The Gene Chip Operating Software (GCOS) absolute analysis algorithm was used to determine the amount of a transcript mRNA (Signal), while the GCOS comparison analysis algorithm was used to compare gene expression levels between two samples.

Present genes were selected as the sequences showing the Detection call 'P' and Signal >100 at least in one sample. Differentially expressed genes were selected as the sequences showing a Change call 'I' or 'D' and Signal Log Ratio >1 or <-1 in the pair-wise comparisons between RLSCs and MMH-D3 cells. The gene list passing this filter was selected as 'changing genes'.

DAVID TOOL 2.1 Beta (http://david.abcc.ncifcrf.gov/) was used to examine selected lists of genes to identify over-representation of functional classes accordingly with gene-ontology (GO) classification.

RNA extraction, reverse transcription, PCR and real time quantitative PCR (RT-qPCR). Total RNA was extracted from cultured cells using an RNA extraction kit (NucleoSpin® RNA II, Machery-Nagel, Germany) according to the manufacturer's instructions. Single-stranded cDNA was obtained by reverse transcription of 1 μg of total RNA using MMLV-reverse-transcriptase (Promega, Italia). cDNA was amplified by PCR using GoTaq enzyme (Promega). RT-qPCRs were performed using BioRad-iQ-iCycler with SYBR green fluorophore; the reactions were carried out using iQ™ SYBR® Green Supermix (BioRad, Hercules, CA, USA); 40 ng of cDNA was used as template and cycling parameters were 95°C for 3 min, followed by 45 cycles of 95°C for 30 s, 60°C for 1 min, 72°C for 30 s, 60°C + 0.5°C for 10 min. Fluorescence intensities were analyzed using the manufacturer's software, and relative amounts were obtained using the $2-\Delta\Delta C_t$ method. For a list of specific primers, see Table 3.

Differentiative culture conditions. All differentiation protocols were performed with three different RLSC lines. The RLSCs hepatocyte differentiation occurs in RPMI-1640, supplemented with 10%FBS, 50 ng/ml EGF, 30 ng/ml IGF-II, 10 μg/ml insulin and antibiotics on collagen-I coated dishes (hepatocyte conditions, HC). Cells were repeatedly grown to confluence and subcultured for 21 days. Medium was changed every 2 days. The RLSCs osteoblast/osteocyte differentiation occurs in DMEM, 10%FBS, 0.1 μM/l dexamethasone, 100 μg/ml ascorbic acid, 10 μM β-glycerol-phosphate (Sigma-Aldrich, St. Louis, MO, USA), 1 μM vitamin A acid (Fluka Riedel-de Haën, Seelze, Germany) on collagen-I coated dishes (osteogenic conditions, OC). 5000 RLSCs/cm^2 were seeded and cultured for 3 weeks. Medium was replenished every 3 days. Osteogenesis was assessed by Alkaline-phosphatase (after 14 days of culture) and red-Alizarin (after 21 days of culture) stainings, in accord with standard protocols. The RLSCs chondrocyte differentiation occurs in the following chondrogenic conditions (CC): 5×10^5

Table 3 List of oligonucleotides used in PCR and in qRT-PCR analyses

Gene	Oligos RT-PCR	Accession no.
β-actin	For 5′-ATGGATGACGATATCGCTGCG-3′ Rev 5′-ATCTTCATGAGGTAGTCTGTCAGG-3′	NM_007393
Liver differentiation		
HNF1	For 5′-CCAACAAGATGTCAGTG-3′ Rev 5′-GCTGGTGAGAGTGTTGATGC-3′	NM_000544
HNF3β	For 5′-ACATGTTCGAGAACGGCTGC-3′ Rev 5′-TGAAGGCTGAATGGTGCTCG-3′	U04197
HNF4	For 5′-ACACGTCCCCATCTGAAG-3′ Rev 5′-CTTCCTTCTTCATGCCAG-3′	NM_008261
E-caderin	For 5′-CAAGCTGGAGACCAGTTTCC-3′ Rev 5′-CAGAGGTGAGCACACTGATG-3′	NM_009864
Transthyretin (TTR)	For 5′-CTGGACTGGTATTTGTGTCT-3′ Rev 5′-TTGGCTGTGAAAACCACATC-3′	NM_013697
Albumin	For 5′-GTGACAAATCCCTTCACACTC-3′ Rev 5′-GTCCTCAACAAAATCAGCAGC-3′	NM_009654
Got1	For 5′-AGCCTCAACCACGAGTACCT-3′ Rev 5′-ATCTGCTTCCACTGCTCTGG-3′	NM_010324
Pepck	For 5′-GACAACTGTTGGCTGGCTC-3′ Rev 5′-GCCCAGGATCAGCATATGC-3′	NM_011044
Eph	For 5′-TGGCTTCAACTCCAGCTACC-3′ Rev 5′-TTCTGACTTGGTCCAGGTGG-3′	NM_010107
α-Fetoprotein (á FP)	For 5′- TCGTATTCCAACAGGAGG-3′ Rev 5′-GAAATCTCACATGGACATC-3′	NM_007423
Chondrogenic differentiation		
Collagen II	For 5′-GATGGCTCTAATGGAATCCC-3′ Rev 5′-CATCGCCATAGCTGAAGTG-3′	NM_031163
Aggrecan	For 5′-GTCTGGAGTAGAAGCTTCAG-3′ Rev 5′-GTAACAGTG ACCCTGGAAC-3′	NM_007424
Osteogenic differentiation		
Osteocalcin	For 5′-AGGACCCTCTCTCTGCTCAC-3′ Rev 5′-GTAGATGCGTTTGTAGGCGGT-3′	NM_04142
Pthr	For 5′-GGGCACAAGAAGTGGATCAT-3′ Rev 5′-GTCCCTGAGACCTCGGTGTA-3′	NM_011199
Periostin	For 5′-AGGTCTCCAAGGTCACAAAG-3′ Rev 5′-TGGACCCAGTCACAATGATG-3′	NM_015784
Osteopontin	For 5′-CAGAGAGCGAGGATTCTGT-3′ Rev 5′-CCAGACTTGGTTCATCCAG-3′	NM_009263
Akp2	For 5′-GACAGCAAGCCCAAGAGACC-3′ Rev 5′-AGAGCGAAGGGTCAGTCAGG-3′	NM_007431
Ibsp	For 5′-GGAGACTTCAAACGAAGAGG-3′ Rev 5′-GTGGTTCCTTCTGCACCTG-3′	NM_008318
Neuronal differentiation		
Nestin	For 5′-AGACACCTGGAAGAAGTTCC-3′ Rev 5′-GGATCATCAGGGAAGTGGTC-3′	NM_016701
Neurogenin1	For 5′-ACCTGCATCTCTGATCTCG-3′ Rev 5′-GATGTAGTTGTAGGCGAAGC-3′	NM_010896
Npas1	For 5′-ACTGGTTACTACCGTTGGCT-3′ Rev 5′-ATACATCAGGCTCAACTCCG-3′	NM_008718
NeuroD2	For 5′-CGAGAAGATTCCTCTTCTCC-3′ Rev 5′-ACAGAGTCTGCACGTAGGT-3′	NM_010895
NeuroD4	For 5′-CGGAACCTTAACTGAAGAGC-3′ Rev 5′-GCTGTGGACAGAGATAGTAG-3′	NM_007501
Fgf9	For 5′ -TGGATATACCTCGCCTAGTG-3′ Rev 5′-TTTCTGGTGCCGTTTAGTCC-3′	NM_013518
Gene	**Oligos RT-PCR**	**Accession no.**
β-actina	For 5′-ACCACACCTTCTACAATGAG-3′ Rev 5′- AGGTCTCAA ACATGATCTGG-3′	NM_007393
Smarcd3	For 5′- ACAGTAAGATCCATGAGACGA-3′ Rev 5′- CACATCTGTCATCACCTTGAG-3′	NM_025891
Foxa1	For 5′- GACCCGTGCTAA ATACTTCC-3′ Rev 5′- TATGTGGTTGGTTTGGTGTG-3′	NM_008259
Nestin	For 5′- ATCCAGAGTTACCAAAGCCT -3′ Rev 5′- GTCTCCAGTGATTCTATGTTCTC-3′	NM_016701
Cnn1	For 5′- AAACAAGAGCGG AGATTTGAG-3′ Rev 5′-CCAGTTTGGGATCATAGAGG-3′	NM_009922
Fzd1	For 5′- GGCACTAAGAAAGAAGGCTG-3′ Rev 5′-ATGGAAATACTGTGAGTTGGC-3′	NM_021457

Table 3 *(Continued)*

Gene	Oligos RT-PCR	Accession no.
Twist2	For 5′-TTCACATCCTCCTCAGATACC-3′ Rev 5′-ATTCCTGAAGCTAGAACTTTCC-3′	NM_007855
Cdh3	For 5′-CTCTTCACTTAGACACTTCTTCC-3′ Rev 5′-AAAGATGATATTCGGCTGCT-3′	NM_007665

trypsinized RLSCs were transferred into a 15-ml polypropylene tube and centrifuged at 1000 r.p.m. for 5 min. The pellet was cultured in chondrogenic medium for 3 weeks. Chondrogenic medium: DMEM, 1% FBS, 37.5 μg/ml ascorbic acid, ITS-premix (BD Biosciences, Bedford, MA, USA) and 10 ng/ml transforming-growth-factor-β1 (PeproTech). The medium was changed every 3 days. Pellets were fixed and sections were stained with alcian blue and immunostained for collagen-type-II (Mouse anti-collagen type-II monoclonal antibody, Chemicon International Inc., Temecula, CA, USA). The RLSCs neural differentiation occurs in the following neurogenic conditions (NC): cells were plated in untreated tissue culture dishes (TechnoPlastic-Products, Trasadingen, Switzerland) in the Advanced-DMEM-F12 medium (Gibco) supplemented with retinoic acid 1ng/ml (Fluka Riedel-de Haën, Seelze, Germany), EGF 20 ng/ml, bFGF 10 ng/ml (PeproTech) and eparin 5ng/ml (Sigma). In these conditions, RLSCs proliferate like spheres. After 6 days these were mechanically dissociated into a single cell suspension and plated at low density on 35 mm Petri dishes coated with Matrigel-Matrix (Becton-Dickinson, San Jose, CA, USA) or with collagen type-I. To induce the differentiation, EGF and bFGF were replaced by 5% FBS for 14 days. The medium was changed every 2 days.

Immunofluorescence and FACS. For indirect immunofluorescence analysis, cells were grown on collagen-I or matrigel-coated dishes, fixed and treated as described previously.[27] The antibodies were used at the following dilutions: mouse monoclonal anti-ZO-1 antibody 1/30 (Zymed-Laboratories, South San Francisco, USA); mouse monoclonal anti-E-cad antibody 1/100 (Transduction Laboratories, BD Biosciences Pharmingen, Palo Alto, CA, USA); rabbit polyclonal anti-Albumin 1/200 (Novus Biologicals Inc. Littleton, CO, USA), goat polyclonal anti-HNF4-alpha 1/100 (c-19) (Santa Cruz Biotechnology, Santa Cruz, CA, USA), rabbit polyclonal anti-GFAP 1/300 (DakoCytomation, Glostrup, Denmark), mouse monoclonal anti Neuronal Class III β-Tubulin 1/500 (Covance, Berkeley, CA, USA). Secondary antibodies (Alexa-Fluor 488 diluted 1:1000) were from Molecular Probes, Eugene, OR, USA. Preparations were examined with a Zeiss Axiophot microscope and with a Leica TCS2 confocal microscope. Flow cytometry was undertaken using a FACS Calibur (Becton Dickinson). Antibodies for flow cytometry analysis: monoclonal antibodies FITC-conjugated anti-CD34 and anti-Sca1; PerCp-conjugated anti-CD90, PE-Cy5-conjugated anti-CD45 and PE-conjugated anti-CD117 were all purchased from BD PharMingen (Erembodegem, Belgium). The biotinylated anti-CD105 and FITC-conjugated anti-CD133 was obtained from eBioscience (San Diego, CA, USA).

Preparation of neovascularized subcutaneous cavity and hepatocyte implantation. To induce neovascularization, osmotic pumps (Alzet, Company, Cupertino, CA, USA) filled with 10 μg of bFGF and 0.1 mg of heparin in 100 μl were implanted into the subcutaneous space on the back of Nu/Nu nude mice (Charles-River Laboratories, Lecco, Italy). Ten days after implantation, when the subcutaneous tissues around the device were efficiently neovascularized, the pumps were removed. Immediately after the removal of the device, 1×10^6 RLSCs, resuspended in an equal mixture of HC medium and Matrigel (BD, Bioscience), were implanted into the subcutaneous pocket. Mice were killed 30 days after cell transplantation and the engineered tissues removed, mounted onto OCT, frozen in liquid propane and cooled by liquid nitrogen. The histological slides were immunostained for Albumin (rabbit polyclonal anti-Albumin, Novus-Biologicals) and cyto-keratin-7 (AbCam, Cambridge, UK).

Acknowledgements. Financial supports: Associazione Italiana per la Ricerca sul Cancro; Ministero della Salute; Ministero dell'Università e della Ricerca Scientifica.

1. Min JY, Sullivan MF, Yang Y, Zhang JP, Converso KL, Morgan JP *et al.* Significant improvement of heart function by cotransplantation of human mesenchymal stem cells and fetal cardiomyocytes in postinfarcted pigs. *Ann Thorac Surg* 2002; **74**: 1568–1575.
2. Liechty KW, MacKenzie TC, Shaaban AF, Radu A, Moseley AM, Deans R *et al.* Human mesenchymal stem cells engraft and demonstrate site-specific differentiation after *in utero* transplantation in sheep. *Nat Med* 2000; **6**: 1282–1286.
3. Lawson DA, Xin L, Lukacs RU, Cheng D, Witte ON. Isolation and functional characterization of murine prostate stem cells. *Proc Natl Acad Sci USA* 2007; **104**: 181–186.
4. Orlic D, Kajstura J, Chimenti S, Jakoniuk I, Anderson SM, Li B *et al.* Bone marrow cells regenerate infarcted myocardium. *Nature* 2001; **410**: 701–705.
5. Pellegrini G, Traverso CE, Franzi AT, Zingirian M, Cancedda R, De Luca M. Long-term restoration of damaged corneal surfaces with autologous cultivated corneal epithelium. *Lancet* 1997; **349**: 990–993.
6. Sangwan VS, Vemuganti GK, Singh S, Balasubramanian D. Successful reconstruction of damaged ocular outer surface in humans using limbal and conjuctival stem cell culture methods. *Biosci Rep* 2003; **23**: 169–174.
7. Fisher RA, Strom SC. Human hepatocyte transplantation: worldwide results. *Transplantation* 2006; **82**: 441–449.
8. Lemire JM, Shiojiri N, Fausto N. Oval cell proliferation and the origin of small hepatocytes in liver injury induced by D-galactosamine. *Am J Pathol* 1991; **139**: 535–552.
9. Lazaro CA, Rhim JA, Yamada Y, Fausto N. Generation of hepatocytes from oval cell precursors in culture. *Cancer Res* 1998; **58**: 5514–5522.
10. Spagnoli FM, Amicone L, Tripodi M, Weiss MC. Identification of a bipotential precursor cell in hepatic cell lines derived from transgenic mice expressing cyto-Met in the liver. *J Cell Biol* 1998; **143**: 1101–1112.
11. Fougere-Deschatrette C, Imaizumi-Scherrer T, Strick-Marchand H, Morosan S, Charneau P, Kremsdorf D *et al.* Plasticity of hepatic cell differentiation: bipotential adult mouse liver clonal cell lines competent to differentiate *in vitro* and *in vivo*. *Stem Cells* 2006; **24**: 2098–2109.
12. Shafritz DA, Oertel M, Menthena A, Nierhoff D, Dabeva MD. Liver stem cells and prospects for liver reconstitution by transplanted cells. *Hepatology* 2006; **43**: S89–98.
13. Petersen BE, Bowen WC, Patrene KD, Mars WM, Sullivan AK, Murase N *et al.* Bone marrow as a potential source of hepatic oval cells. *Science* 1999; **284**: 1168–1170.
14. Theise ND, Badve S, Saxena R, Henegariu O, Sell S, Crawford JM *et al.* Derivation of hepatocytes from bone marrow cells in mice after radiation-induced myeloablation. *Hepatology* 2000; **31**: 235–240.
15. Theise ND, Nimmakayalu M, Gardner R, Illei PB, Morgan G, Teperman L *et al.* Liver from bone marrow in humans. *Hepatology* 2000; **32**: 11–16.
16. Vassilopoulos G, Wang PR, Russell DW. Transplanted bone marrow regenerates liver by cell fusion. *Nature* 2003; **422**: 901–904.
17. Wang X, Willenbring H, Akkari Y, Torimaru Y, Foster M, Al-Dhalimy M *et al.* Cell fusion is the principal source of bone-marrow-derived hepatocytes. *Nature* 2003; **422**: 897–901.
18. Vig P, Russo FP, Edwards RJ, Tadrous PJ, Wright NA, Thomas HC *et al.* The sources of parenchymal regeneration after chronic hepatocellular liver injury in mice. *Hepatology* 2006; **43**: 316–324.
19. Dan YY, Riehle KJ, Lazaro C, Teoh N, Haque J, Campbell JS *et al.* Isolation of multipotent progenitor cells from human fetal liver capable of differentiating into liver and mesenchymal lineages. *Proc Natl Acad Sci USA* 2006; **103**: 9912–9917.
20. Herrera MB, Bruno S, Buttiglieri S, Tetta C, Gatti S, Deregibus MC *et al.* Isolation and characterization of a stem cell population from adult human liver. *Stem Cells* 2006; **24**: 2840–2850.
21. Amicone L, Spagnoli FM, Spath G, Giordano S, Tommasini C, Bernardini S *et al.* Transgenic expression in the liver of truncated Met blocks apoptosis and permits immortalization of hepatocytes. *EMBO J* 1997; **16**: 495–503.
22. Spagnoli FM, Cicchini C, Tripodi M, Weiss MC. Inhibition of MMH (Met murine hepatocyte) cell differentiation by TGF(beta) is abrogated by pre-treatment with the heritable differentiation effector FGF1. *J Cell Sci* 2000; **113** (Part 20): 3639–3647.
23. Strick-Marchand H, Weiss MC. Inducible differentiation and morphogenesis of bipotential liver cell lines from wild-type mouse embryos. *Hepatology* 2002; **36**: 794–804.
24. Peterson CL. Chromatin remodeling enzymes: taming the machines. Third in review series on chromatin dynamics. *EMBO Rep* 2002; **3**: 319–322.

25. Quesenberry PJ, Colvin GA, Lambert JF. The chiaroscuro stem cell: a unified stem cell theory. *Blood* 2002; **100**: 4266–4271.
26. Fry CJ, Peterson CL. Chromatin remodeling enzymes: who's on first? *Curr Biol* 2001; **11**: R185–R197.
27. Mevel-Ninio M, Weiss MC. Immunofluorescence analysis of the time-course of extinction, reexpression, and activation of albumin production in rat hepatoma-mouse fibroblast heterokaryons and hybrids. *J Cell Biol* 1981; **90**: 339–350.

Supplementary Information accompanies the paper on Cell Death and Differentiation website (http://www.nature.com/cdd)